

# Network-Type Modeling of Micromachined Sensor Systems

G. Lorenz and R. Neul

Robert Bosch GmbH, Germany, lorenz@fi.sh.bosch.de, neul@fi.sh.bosch.de

## ABSTRACT

This paper describes the development of network-type models for the simulation of micromechanical components such as spatial beams and masses. The models were coded in MAST<sup>®</sup> for the SABER<sup>®</sup> simulator and their accuracy was compared to analytical solutions and FEM simulations using ANSYS<sup>®</sup>. This approach leads to a library of network-type multi domain component models for the system simulation of MEMS, providing nearly FEM accuracy at network-type simulation speed<sup>1</sup>.

**Keywords:** MEMS, network-type modeling, spatial beam model, SABER, MAST, general motion.

## INTRODUCTION

The design process of commercial MEMS structures today is commonly characterized by a large number of foundry runs and time-consuming experimental set-ups to get a detailed overview of the sensor's behavior. System simulations that include an accurate physical model of the sensor would help to accelerate and improve this process considerably.

The available tools for mechanical simulations can be categorized into field solvers and multi body simulators. The Finite Element codes are the traditional simulators for design investigations on MEMS structures. Due to their high accuracy they are well suited to calculate stress distributions, distortions and natural frequencies of MEMS structures. They are unsuitable, however, to take into account large scale motion. This domain is the traditional area for multi-body simulators. Their internal solving algorithm is based on system energy considerations such as the Lagrange method or the principle of Hamilton. Although well suited for mechanical systems, their intrinsic solver excludes the implementation of other physical domains like electronic circuits or electrostatic fields.

Network simulators offer a more general system description. They are well suited for a building-block-

<sup>1</sup>MAST<sup>®</sup> is a registered trademark of Analogy, Inc. SABER<sup>®</sup> is a registered trademark of American Airlines, Inc., licensed to Analogy, Inc. ANSYS<sup>®</sup> is a registered trademark of ANSYS, Inc.

oriented system simulation. The general approach provides for the decomposition of a complex micro system into simpler basic components.

The objective of the presented paper is to provide basic mechanical elements for a network-type simulator, implemented using an analog behavioral description language. Together with electro-mechanical system components a more complex system e. g. an angular rate sensor) will be composed from basic mechanical elements.

## MODELING OF SPATIAL BEAMS

The description of mechanical beams in the design of MEMS devices are based on finite element analysis. Therefore, the mechanical beam structure is considered to be composed of finite elements. The accuracy of the simulation is determined by the choice of the particular approach and the number of elements used. This modeling approach is based on spatial beam elements. The elastic behavior of a single spatial beam element can be modeled by a stiffness matrix  $\mathbf{K}$ , the damping matrix  $\mathbf{D}$  and the mass matrix  $\mathbf{M}$ .

$${}_b\mathbf{F} = \mathbf{M} {}_b\ddot{\mathbf{x}} + \mathbf{D} {}_b\dot{\mathbf{x}} + \mathbf{K} {}_b\mathbf{x} \quad (1)$$

Linear and angular displacements of the element nodes are comprised in the vector  ${}_b\mathbf{x}$ . Forces and torques acting on the system are represented by vector  ${}_b\mathbf{F}$ . All vectors in (1) are written in a local beam coordinate system (prefix b), see fig. 1. Mass matrix  $\mathbf{M}$  and stiff-

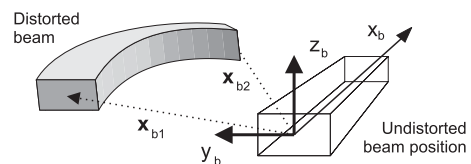


Figure 1: Beam coordinate system

ness matrix  $\mathbf{K}$  can be derived from a continuous beam element. Applying the principle of D'Alembert leads to mass and stiffness matrices depicted in (2) and (3) [1], [2]. The derivation is based on an abstraction, taking into account only the two end points of the beam and the forces and displacements occurring on them.

Torsion, bending and expansion are considered to be independent. Such an approximation is only valid for



$${}_{b_o}T_{b_1} = \begin{bmatrix} \cos \beta_1 \cos \gamma_1 & -\cos \beta_1 \sin \gamma_1 & \sin \beta_1 \\ \cos \alpha_1 \sin \gamma_1 + \sin \alpha_1 \sin \beta_1 \cos \gamma_1 & \cos \alpha_1 \cos \gamma_1 - \sin \alpha_1 \sin \beta_1 \sin \gamma_1 & -\sin \alpha_1 \cos \beta_1 \\ \sin \alpha_1 \sin \gamma_1 - \cos \alpha_1 \sin \beta_1 \cos \gamma_1 & \sin \alpha_1 \cos \gamma_1 + \cos \alpha_1 \sin \beta_1 \sin \gamma_1 & \cos \alpha_1 \cos \beta_1 \end{bmatrix} \quad (5)$$

They are used to define the undistorted position of the beam with respect to the reference system. During the simulation, the mechanical “nodes” hold only the relative motions  $\mathbf{r}_{1d}$  and  $\mathbf{r}_{2d}$  of the beam ends as across variables. The twelve nodes of the network beam, in a reference environment, represent the forces and torques as variables in reference coordinates.

Large geometric excursions applied to acceleration or angular rate sensors can be expressed by a motion of the reference system  $\mathbf{r}_R$  and  $\boldsymbol{\omega}_R$  relative to the inertial coordinate system (see fig. 3). The introduction of ref-

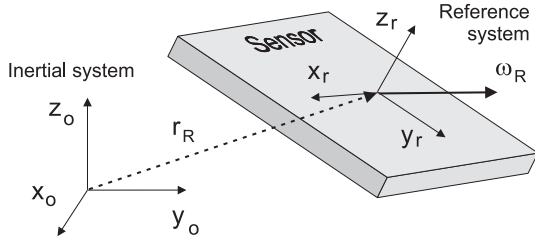


Figure 3: Inertial system

erence coordinates requires additional transformations since (1) is only valid for displacements and forces given in the local beam coordinate system of fig. 1. According to fig. 2 the distorted position of beam end 1 can be determined using:

$$\mathbf{r}_1 = \mathbf{r}_{1o} + \mathbf{r}_{1d} \quad (6)$$

The angular position of beam end 1 can be obtained using Bryant angles  $\alpha_1, \beta_1, \gamma_1$ . The three angles form the transformation matrix  ${}_{b_o}T_{b_1}$  from distorted beam coordinates (index  $b_1$ ) to undistorted beam coordinates (prefix  $b_o$ ). The definition of the transformation matrix  ${}_{b_o}T_{b_1}$  can be seen in (5).

The undistorted beam position is obtained using transformation matrix  ${}_{r}T_{b_o}$ . This matrix can be calculated from the position vectors  $\mathbf{r}_{1o}$  and  $\mathbf{r}_{2o}$  prior to simulation iterations. The transformation matrix  ${}_{r}T_{b_1}$  between beam end 1 and reference system is:

$${}_{r}T_{b_1} = {}_{b_o}T_{b_1} {}_{r}T_{b_o} \quad (7)$$

The position of beam end 2 is obtained likewise. Thus, the position in space of both beam ends can be determined. To simplify further calculations, beam end 1 is chosen as the origin for the local beam coordinate system. Hence, beam end 1 is undistorted by definition, see fig. 4. Then the local position of beam end 2 is given by:

$${}_{b}r_2 = {}_{b_1}r_2 = {}_{b_1}T_r ({}_r r_2 - {}_r r_1) - [l \ 0 \ 0]^T \quad (8)$$

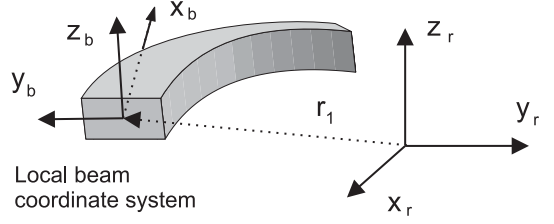


Figure 4: Local beam coordinates

Where  ${}_{b_1}T_r = {}_rT_{b_1}^{-1}$ . The angles between beam end 1 and beam end 2 ( $\alpha_{12}, \beta_{12}, \gamma_{12}$ ), and therefore the angular position of beam end 2 in beam coordinates can be obtained by calculating the transformation  ${}_{b_1}T_{b_2}$ :

$${}_{b_1}T_{b_2} = {}_{b_1}T_{r_r} T_{b_2} \approx \begin{bmatrix} 1 & -\gamma_{12} & \beta_{12} \\ \gamma_{12} + \alpha_{12}\beta_{12} & 1 - \alpha_{12}\beta_{12}\gamma_{12} & -\alpha_{12} \\ \alpha_{12}\gamma_{12} - \beta_{12} & \alpha_{12} + \beta_{12}\gamma_{12} & 1 \end{bmatrix} \quad (9)$$

Leading to a new  ${}_{b}x$ :

$${}_{b}x = [0 \ 0 \ 0 \ 0 \ 0 \ 0 \ {}_{b}r_2^T \ \alpha_{12} \ \beta_{12} \ \gamma_{12}]^T \quad (10)$$

## Damping and inertial properties

The damping of the beam motion is caused by fluid and material damping and is based on the velocity of the movable parts relative to the sensor housing, i. e. the reference system. Therefore, the derivative of  ${}_{b}x$  relative to the reference system has to be obtained.

However, the absolute second derivative of  ${}_{b}x$  relative to the inertial frame is needed to calculate the inertial beam properties.

The absolute linear and angular acceleration of a body in a reference system [1] is given by :

$$\mathbf{a}(t) = \overset{*}{\ddot{\mathbf{r}}}_R + \left( \overset{\cdot}{\dot{\boldsymbol{\omega}}}_R + \tilde{\boldsymbol{\omega}}_R^2 \right) \mathbf{r}_r + 2\tilde{\boldsymbol{\omega}}_R \dot{\mathbf{r}}_r + \ddot{\mathbf{r}}_r \quad (11)$$

$$\boldsymbol{\alpha}(t) = \dot{\boldsymbol{\omega}}_R + \tilde{\boldsymbol{\omega}}_R \boldsymbol{\omega}_r + \dot{\boldsymbol{\omega}}_r \quad (12)$$

Where (\*) is the derivative in the inertial system and (·) the derivative in the reference system. Vector  $\mathbf{r}_R$  is the vector between inertial and reference system and  $\boldsymbol{\omega}_R$  the angular velocity of the reference system (see fig. 3). Furthermore, the position of the body in the reference system is given by  $\mathbf{r}_r$  and its angular velocity by  $\boldsymbol{\omega}_r$ . ( $\tilde{\mathbf{a}}\mathbf{b}$  means  $\mathbf{a} \times \mathbf{b}$ ).

Equations (11) and (12) can be expressed in any coordinate system. Here we need both equations expressed in the reference system.

According to [1] the angular velocity of beam end 1 in the reference system can be expressed by:

$${}_{r}\tilde{\boldsymbol{\omega}}_1 = {}_r\dot{T}_{b_1} {}_{b_1}T_r \quad (13)$$

The absolute linear and angular accelerations of beam end 2 are calculated likewise. This leads to the second derivative of  ${}_b\mathbf{x}$ :

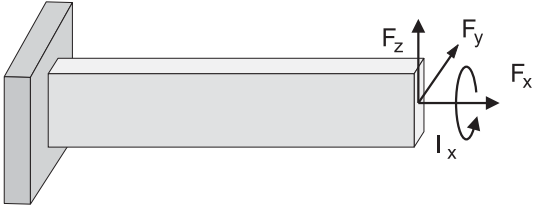
$${}_b\ddot{\mathbf{x}} = [{}_bT_{rr}\mathbf{a}_1^T \quad {}_bT_{rr}\mathbf{\alpha}_1^T \quad {}_bT_{rr}\mathbf{a}_2^T \quad {}_bT_{rr}\mathbf{\alpha}_2^T]^T \quad (14)$$

Equation (11) and (12) contain the time dependent variables of the inertial motion of the reference system  ${}^{**}\mathbf{r}_R$  and  $\boldsymbol{\omega}_R$ . Thus, they have to be supplied as an additional input to each beam template with inertial properties.

Using the presented theory, we can use (1) to model a network-type beam referenced in a moving coordinate system which is fixed to the sensor's housing.

## Verification of the beam model

A verification of the modeling approach was carried out using a simple cantilever beam. This test beam



Height of the beam	h	=	5.0 $\mu\text{m}$
Width of the beam	w	=	0.2 $\mu\text{m}$
Length of the beam	l	=	160 $\mu\text{m}$
Density	$\rho$	=	2326 $\text{kg}/\text{m}^3$
Modulus of elasticity	E	=	1.302 $10^{11}$ $\text{N}/\text{m}^2$
Modulus of shear	G	=	79.62 $10^9$ $\text{N}/\text{m}^2$
Mass	m	=	3.7216 $10^{-13}$ $\text{kg}$

Figure 5: Cantilever beam for verification purposes

is shown in fig. 5. This simple structure was chosen, because it is possible to obtain an analytical solution as a reference. Therefore, the natural frequencies of the beam have been calculated analytically ([4], [5]).

The longitudinal vibration is described by the partial differential equation:

$$\frac{\partial^2}{\partial t^2}w_x(x,t) = \frac{E}{\rho} \frac{\partial^2}{\partial x^2}w_x(x,t) \quad (15)$$

$w_x(x,t)$  is the longitudinal displacement. Considering the special boundary conditions in this case, one can obtain the well known natural frequencies:

$$\omega_k = \left(k - \frac{1}{2}\right) \frac{\pi}{L} \sqrt{\frac{E}{\rho}} \quad k = (1, 2, \dots) \quad (16)$$

Bending vibrations are described by:

$$\frac{\partial^2}{\partial t^2}w_y(x,t) = -\frac{EJ_y}{\rho A} \frac{\partial^4}{\partial x^4}w_y(x,t) \quad (17)$$

$w_y(x,t)$  is the lateral displacement in y-direction. Using  $J_z$  instead of  $J_y$  yields to the lateral displacement

$w_z(x,t)$  in z-direction. Boundary conditions result in the eigenvalue equation  $\cosh\lambda_k \cos\lambda_k = -1$  for the spatial eigenvalues  $\lambda_k$ . Taking the solutions  $\lambda_k$ , the natural frequencies are:

$$\omega_k = \sqrt{\frac{EJ_y}{\rho A}} \frac{\lambda_k^2}{L^2} \quad k = (1, 2, \dots) \quad (18)$$

Torsional vibrations are described by:

$$\frac{\partial^2}{\partial t^2}\varphi(x,t) = -\frac{GJ_t}{\rho J_p} \frac{\partial^2}{\partial x^2}\varphi(x,t) \quad (19)$$

$\varphi(x,t)$  is the angular displacement. Natural frequencies are:

$$\omega_k = \left(k - \frac{1}{2}\right) \frac{\pi}{L} \sqrt{\frac{GJ_t}{\rho J_p}} \quad k = (1, 2, \dots) \quad (20)$$

ANSYS-simulations of the beam were also done for comparison, using spatial beam elements from ANSYS respectively. The beam was subdivided into 100 elements along its length. With the calculated frequencies it was tested how close the generated SABER models match the natural frequencies of vibration. Therefore, AC-analyses were performed. Table 6 compares the natural frequencies calculated by ANSYS, the natural frequencies of the provided SABER models and the natural frequencies of the analytical solution. The state errors are always with respect to the analytical solution.

In the SABER simulation run, the beams with 2, 4 and 8 elements were stimulated using sinusoidal forces  $F_y$ ,  $F_z$  and torques  $I_x$ . Because, the center line of the proposed network beam element is modeled as a cubic function in space, a single element can only reproduce the first bending mode. For every further mode an additional beam element has to be added.

Using this technique, the calculated frequencies of the network model correspond very well to the analytical solutions. Furthermore, the proposed beam model includes the properties to account for Coriolis and other inertial forces and torques caused by the motion of the reference system as well as internal sensor forces such as electrostatic forces.

## MODELING OF RIGID BODIES

It is not always necessary to model all bodies with elastic properties. For large masses in acceleration or angular rate sensors it's a good approximation to consider them as rigid. This approximation can improve simulation speed considerably without sacrificing much accuracy.

The properties of a rigid body in space are determined by its mass  $m$  and its moment of inertia  $\mathbf{J}$ . The forces  $\mathbf{F}$  and torques  $\mathbf{I}$  acting on a rigid body are given by the equations of momentum and angular momentum:

$$\mathbf{F}(t) = m\mathbf{a}(t) \quad (21)$$

Mode	Stim.	Analytic Solution [kHz]	ANSYS (100 elements) [kHz]		SABER (2 elements) [kHz]		SABER (4 elements) [kHz]		SABER (8 elements) [kHz]	
1.	$F_y$	9.4458	9.438	0.08%	9.447	0.013%	9.442	0.04%	9.442	0.04%
2.	$F_y$	59.196	59.143	0.09%	59.67	0.8%	59.24	0.07%	59.18	0.03%
3.	$F_y$	165.750	165.606	0.09%			166.97	0.73%	165.79	0.02%
4.	$F_z$	236.144	236.007	0.06%	236.2	0.02%	236.02	0.05%	236.0	0.06%
5.	$F_y$	324.803	324.539	0.08%			329.39	1.39%	325.40	0.18%
6.	$F_y$	536.923	536.564	0.07%					539.82	0.54%
7.	$I_x$	721.484	731.106	1.219%	740.14	2.52%	726.13	0.64%	722.70	0.17%
8.	$F_y$	802.070	801.737	0.04%					811.28	1.14%
9.	$F_y$	1120.25	1120.0	0.02%					1142.1	1.91%
10.	$F_z$	1479.89	1480.0	0.01%	1485.6	0.38%	1478.7	0.08%	1477.8	0.14%
11.	$F_y$	1491.45	1519.8	1.90%					1517.2	1.7%

Figure 6: Modal analysis

$$\mathbf{I}(t) = \mathbf{J}(t)\boldsymbol{\alpha}(t) + \tilde{\boldsymbol{\omega}}(t)\mathbf{J}(t)\boldsymbol{\omega}(t) \quad (22)$$

Using (21) and (11), we get suitable equations for calculating the forces acting on a rigid body. All vectors are expressed in the already introduced reference system (see fig. 2).

$${}_r\mathbf{F} = m \left( {}_r\ddot{\mathbf{r}}_R + ({}_r\dot{\boldsymbol{\omega}}_R + {}_r\tilde{\boldsymbol{\omega}}_R^2) {}_r\mathbf{r}_r + 2 {}_r\tilde{\boldsymbol{\omega}}_R {}_r\dot{\mathbf{r}}_r + {}_r\ddot{\mathbf{r}}_r \right) \quad (23)$$

Vector  ${}_r\mathbf{r}$  defines the linear position of the mass with respect to the reference system.

Equations (21) and (22) are valid in any coordinate system. Equation (22) however, should be expressed in a coordinate system which is fixed to the mass itself. The coordinate system fixed to the mass (prefix m) is the only one in which the matrix of the moments of inertia  $\mathbf{J}$  is time independent.

$${}_r\mathbf{I} = {}_rT_m ({}_m\mathbf{J} {}_m\boldsymbol{\alpha} + {}_m\tilde{\boldsymbol{\omega}} {}_m\mathbf{J} {}_m\boldsymbol{\omega}) \quad (24)$$

${}_rT_m$  describes the coordinate transformation from mass to reference coordinates and is a function of the position angles  $(\alpha, \beta, \gamma)$ .

The disadvantages of a mass coordinate system are the necessary transformations for the absolute angular velocity  ${}_m\boldsymbol{\omega}$  and acceleration  ${}_m\boldsymbol{\alpha}$ .

$${}_m\boldsymbol{\omega} = {}_rT_m^{-1} {}_r\boldsymbol{\omega}_R + {}_m\boldsymbol{\omega}_r \quad (25)$$

$${}_m\boldsymbol{\alpha} = {}_m\dot{\boldsymbol{\omega}}_R + {}_m\tilde{\boldsymbol{\omega}}_R {}_m\boldsymbol{\omega}_r + {}_m\dot{\boldsymbol{\omega}}_r \quad (26)$$

The angular velocity  ${}_m\boldsymbol{\omega}_r$  of the body with respect to the mass coordinate system can be calculated directly using the angles  $\alpha$ ,  $\beta$  and  $\gamma$  connected to the mass model.

$${}_m\boldsymbol{\omega}_r = \begin{bmatrix} \cos \beta \cos \gamma & \sin \gamma & 0 \\ -\cos \beta \sin \gamma & \cos \gamma & 0 \\ \sin \beta & 0 & 1 \end{bmatrix} \begin{bmatrix} \dot{\alpha} \\ \dot{\beta} \\ \dot{\gamma} \end{bmatrix} \quad (27)$$

In contrast to the previously described beam model, the network model of a rigid body needs only six mechanical wires, representing the six degrees of freedom as across (node) variables and the corresponding torques and forces as through (conserved) variables. In addition, we need again the knowledge of the motion of the reference system  ${}_r\mathbf{r}^{**}$  and  ${}_r\boldsymbol{\omega}_R$  with respect to the inertial frame in reference coordinates. Thus, we define six visible “wires” for the position in reference coordinates and six invisible “wires” for the inertial motion.

## SENSOR EXAMPLE

A recent design of an angular rate sensor shall serve as an example to demonstrate the idea of a network-type system model of MEMS structures. The SEM

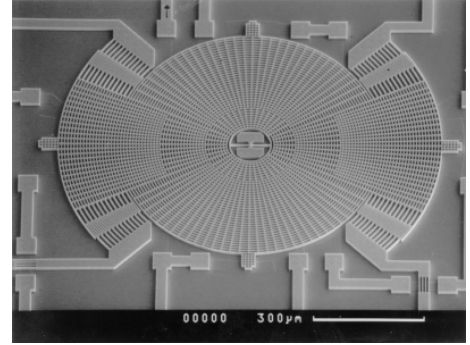


Figure 7: SEM of an angular rate sensor structure

image fig. 7, shows an angular rate sensor design, recently under investigation at the BOSCH research laboratories. The mechanical sensor consists primarily of a flat movable polysilicon structure which is suspended by two beams in the center of the element. The “rotor” can be driven into resonant vibration about the vertical axis by four comb drives located on the outer edge of the structure. If an angular velocity is applied perpendicular

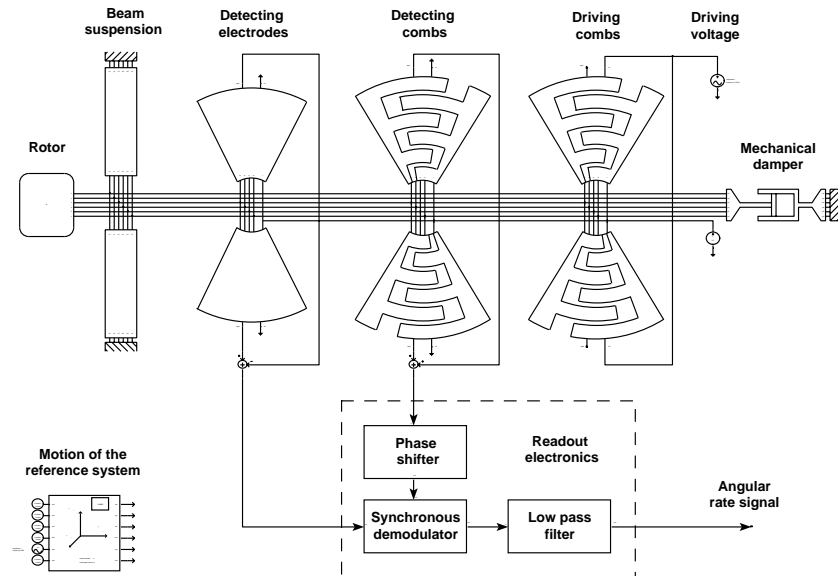


Figure 8: SABER system model of an angular rate sensor

lar to the vertical axis, the rotor responds with a tilting oscillation due to the principle of conservation of angular momentum. The tilt oscillation has the frequency of the in-plane motion and an amplitude proportional to the applied angular rate. This motion can be detected by underlying electrodes.

The whole sensor system, including readout electronics, can be modeled using a network simulation tool. Fig. 8 shows a SABER model composed of reusable electro mechanical components. The rotor is modeled as the above described rigid body. Each of the two beams, which form the rotor suspension, consists of two beam elements. In addition to the six terminals, which connect the beam and mass symbols, there are six invisible “wires”. These wires carry the information of the sensor motion in the inertial frame to every symbol with inertial properties. They have their origin in the symbol “Motion of the reference system”.

Symbols for the detecting electrodes, comb drives, damper and readout electronics complete the model of the angular rate sensor.

## CONCLUSIONS

The applicability of the introduced modeling approach to include mechanical components into the system simulation with SABER was shown using an angular rate sensor as an example. The approach gives an accurate description of the complex static and dynamic behavior of mechanical structures composed of spatial beams and rigid body elements. The application of the described methods in addition to electrostatic comb drives and capacitive readout circuits is discussed in a separate publication [6].

## ACKNOWLEDGMENTS

The authors would like to acknowledge P. Schwarz, J. Haase and S. Reitz (FhG-IIS/EAS, Dresden, Germany) for their helpful contributions. Furthermore, we would like to thank U. Becker and S. Götz (Robert Bosch GmbH, Germany) and last but not least Darrell Teegarden (Analogy Inc., USA) for very helpful programming details.

This work was partly supported by the German government, Dept. of Education and Research (BMBF), under grant number 16SV236/0.

## REFERENCES

- [1] W. Schielen, *Technische Dynamik*. Stuttgart: Teubner, 1986.
- [2] J. S. Przemieniecki, *Theory of Matrix Structural Analysis*. Dover, 1985.
- [3] R. Neul, U. Becker, G. Lorenz, P. Schwarz, J. Haase, and S. Wünsche, “A modeling approach to include mechanical microsystem components into the system simulation,” in *DATE’98 - Design, Automation and Test in Europe*, vol. 1, pp. 510–517, Feb 1998.
- [4] E. W. Beitz and K.-H. Küttner, *Dubbel – Taschenbuch für den Maschinenbau*. Springer Verlag, 1990.
- [5] H. H. Woodson and J. R. Melcher, *Electromechanical Mechanics*. New York: John Wiley & Sons, 1968.
- [6] G. Lorenz and R. Neul, “Integration von mikrosystemtechnischen Komponenten in die Netzwerk- und Systemsimulation am Beispiel eines Drehratensensors,” in *Proc. 6. Workshop: Methoden und Werkzeuge zum Entwurf von Mikrossystemen*, vol. 1, pp. 39–46, Dez 1997.